AIMS Mathematics, 7(5): 8290–8313.
DOI: 10.3934/math.2022462
Received: 27 December 2021
Revised: 05 February 2022
Accepted: 13 February 2022
Published: 25 February 2022

http://www.aimspress.com/journal/Math

Research article

Nonlinear wave train in an inhomogeneous medium with the fractional theory in a plane self-focusing

Muhammad Imran Asjad[1], Waqas Ali Faridi[1], Adil Jhangeer[2], Maryam Aleem[1], Abdullahi Yusuf[3,4*], Ali S. Alshomrani[5] and Dumitru Baleanu[6,7,8]

[1] Department of Mathematics, University of Management and Technology, Lahore, Pakistan
[2] Department of Mathematics, Namal Institute, Talagang Road, Mianwali 42250, Pakistan
[3] Department of Computer Engineering, Biruni University, Istanbul, Turkey
[4] Department of Mathematics, Near East University TRNC, Mersin 10, Turkey
[5] Department of Mathematics, King Abdul Aziz University, Jeddah, Saudi Arabia
[6] Department of Mathematics, Cankaya University, Ankara, Turkey
[7] Institute of Space Sciences, Magurele, Bucharest, Romania
[8] Department of Medical Research, China Medical University, Taichung, Taiwan

* **Correspondence:** Email: ayusuf@biruni.edu.tr; Tel: +905343635957.

Abstract: The aim of study is to investigate the Hirota equation which has a significant role in applied sciences, like maritime, coastal engineering, ocean, and the main source of the environmental action due to energy transportation on floating anatomical structures. The classical Hirota model has transformed into a fractional Hirota governing equation by using the space-time fractional Riemann-Liouville, time fractional Atangana-Baleanu and space-time fractional β differential operators. The most generalized new extended direct algebraic technique is applied to obtain the solitonic patterns. The utilized scheme provided a generalized class of analytical solutions, which is presented by the trigonometric, rational, exponential and hyperbolic functions. The analytical solutions which cover almost all types of soliton are obtained with Riemann-Liouville, Atangana-Baleanu and β fractional operator. The influence of the fractional-order parameter on the acquired solitary wave solutions is graphically studied. The two and three-dimensional graphical comparison between Riemann-Liouville, Atangana-Baleanu and β-fractional derivatives for the solutions of the Hirota equation is displayed by considering suitable involved parametric values with the aid of Mathematica.

Keywords: multi-wave non-linear Hirota equation; fractional derivatives; travelling wave transformation; new extended direct algebraic method; soliton solutions
Mathematics Subject Classification: 34K25, 34K40, 37B25, 58K25

1. Introduction

Ordinary differential equations are equations involving a single variable whereas partial differential equation (PDE) involves two or more variables. There is a significant development in the field of differential equations during the 20th century. The major reason behind this is ever-increasing mathematical applications in the field of medicine, engineering, computer technology, mathematical biology, aerodynamics, etc. All physical processes are described mathematically by non-linear PDEs. Fractional differential equations (FDEs) are the generalization of ODEs and have magnanimous applications in quantum mechanics, solid-state physics, ultrasonography, signal processing, mathematical biology, physics, fractional dynamics, finance, engineering, control theory, and have progressively captivated the attention of researchers due to immense applications. Recent work on FDEs can be seen in [1–5]. To accomplish analytical as well as exact solutions of traveling waves traced by nonlinear fractional differential equations is a major contribution in nonlinear sciences since it portrays mixed natural processes like solitons, vibrations and speed distribution. FDEs remove the constraints of locality and provide in-depth knowledge about system mechanism [6]. Solitons are the solutions of non-linear diffusive PDEs describing any tangible systems. John Scott Russel (1808–1882) was the first one who described the phenomenon of soliton in 1834 and detected a soliton wave in the Union Canal in Scotland. In mathematics and physics, a solitary wave or soliton is just like a spiral wave bundle that preserves its shape when it spreads at an invariant velocity [7,8]. All real-world processes are described with the help of PDEs, constituting a complicated set of problems that might not be solved exactly but their analytical solutions can be achieved by keeping in mind their practical scenarios and theoretic prospects. Many efficient techniques demonstrated in the literature, are applied to investigate exact or analytic solutions of PDE.

To explore the dynamic behavior of tangible real systems is always an active research domain for mathematicians in every era. During the 20th-century, researchers started inquiring in-depth analysis of non-linear systems and their centripetal compositions and considerable attention was paid to Chaos theory which states that PDEs and ODEs could demonstrate unbelievably plenteous behavior, permitting around settled schemes to be exponentially episodic for flaring time. Soliton theory enables mathematicians to vouch for the stable behavior of non-linear PDEs (systems) in a quasi-linear manner. Atangana and Seda modeled Labyrinth chaotic problems with fractional operators which include power law, exponential decay and Mittag-Leffler kernel. The mathematical model is worked out through a numeric scheme named Atangana-Seda established on Newton polynomial [9].

In another manuscript, they've formulated a COVID-19 spread mathematical model in South Africa and Turkey, portrayed statistical analysis, applied optimal theory [10] and modified numerical scheme [11]. In another article, they have studied three epidemiologic troubles, incorporating the zika and zombie virus spread model and Ebola model. The solution of these models is obtained by the proposed numeric scheme [12]. Mirzazadeh had obtained a one-soliton solution by employing 1st integral and complex fractional transformed method to time-dependent parabolic fractional-order PDE [13]. Tebue et al. had acquired the soliton solutions of fractional non-linear Zoomeron equations and illustrated that these results could explain numerous phenomena in optics, lasers as well as in fluid mechanics [14]. Tebue et al. studied the nonlinear Schrodinger equation and obtained exact analytical results by acquiring two advances: (i) nonlinear impulsive parameters and (ii) new Jacobi elliptic function expansion technique. The dynamics of solitary wave optic proclamation had been discovered

in mono-mode optical fibers [15].

Zayed et al. has made the group analysis to work out soliton and invariant solutions of Euler non-linear PDEs by using extended modified Tanh-function [16]. The solutions of traveling waves representing the Schrodinger equation in non-Kerr law media were investigated by Biswas et al. [17]. They had obtained optical perturbed solitons with the help of perturbation theory. Solitary solutions commonly appear in nature. The mathematical description of these wave solutions is a remarkable achievement of researchers and mathematicians. These solutions represent kink-shaped or dark solitons which are tangent hyperbolic results, bell-shaped (secant hyperbolic expressions) [18]. Soliton solutions were obtained by applying various method like, tangent hyperbolic (extended function) [19], 1st integral method [20], the Darboux transformation process [21], F-expansion technique [22]. In all these methods non-linear PDEs were expressed in terms of the set of algebraic equations by adapting the balancing terms approach and their solutions yield explicit wave expressions.

Some recent research papers are presented here. Akinyemi et al. [23] applied three distinct techniques which are $\frac{G'}{G}$, Riccati and Kudryashov method, and obtained soliton solutions for conformable Schrödinger (NLCS) system of equations. Akbar et al. [24] acquired kink, bell-type, anti-bell type solitons and compactons for the Boussinesq equation by using the generalized Kudryashov and sine Gorden method. Akinyemi et al. [25] analyzed the bright and singular solitons of the nonlinear Schrödinger equation. Akinyemi et al. [26] investigated the solitons with parabolic non-linearity by using the auxiliary equation method. Mirzazadeh et al. [27] studied the solitary wave solutions of perturbed Biswas-Milovic equation with the aid of Kudryashov's law of refractive index. Kilicman et al. [28] studied the analytical solutions of the M-Burgers fractional equation by using the homotopy perturbation method. Shokhanda et al. [29] established the analytical approximation for the time-fractional two-mode couple Burger equation with the aid of the modified homotopy perturbation method. Yuan et al. [30] presented the multiple solitons for discrete nonlocal nonlinear self-dual network equation by using nonlocal discrete N-fold Darboux transformation. Wang and Wen [31] investigated the semi-discrete two-component integrable system on zigzag runged ladder lattice and obtained a variety of two-component localized waves. Yuan and Wen [32] analyzed discrete modified exponential Toda lattice equation by using the Darboux transformation and acquired soliton solutions. Wen and Wang [33] constructed generalized Darboux transformation and obtained solutions of coupled Ablowitz-Ladik equations. Wang et al. [34] investigated the Hirota coupled system with variable coefficients and obtained rogue waves by using the Darboux transformation and also provided modulation instability. Wang et al. [35] considered coupled Biswas-Milovic (CMB) system and applied n-fold Darboux transformation to get a generalized solution of the system.

The multi-wave non-linear Hirota equation is an integral conjecture of the Schrodinger wave equation that illustrates ultra-short beats due to higher-order dissemination and self-steepening impression [36]. It is significant in the domain of mathematical and theoretical physics. This non-linear differential equation traces the generation of femtosecond solitonic pulse in a single-phase mode fiber. Subsequently, the multitudinous, schnorkels, rogue waving and varlet higher-order waves for Hirota equation [37] was speculated by numerous analysts through generalized Darboux transformation technique and other ways [38, 39].

El-Rashidy [40] studied the Hirota equation and discussed a few soliton solutions and their interaction, but a lot of solitons types were still missed. El-Rashidy just discussed the kinky type solitons and their interaction but dark, bright, singular, rational, periodic, dark-bright, dark singular,

bright singular and periodic type solitons, etc., were missed. Therefore, to fulfill this gap, the authors tried to establish this study and to find others types of solitons. The other most significant gap was that the existed study in literature was done with the classical theory of differentiation, which is a local theory, authors also tried to develop solitons with the fractional theory of calculus which is a generalization and global theory. The multi-wave non-linear Hirota equation in [41]:

$$i\frac{\partial Q}{\partial t} + \beta\frac{\partial^2 Q}{\partial x^2} + \delta Q|Q|^2 + i\gamma\frac{\partial^3 Q}{\partial x^3} + 3i\lambda\frac{\partial Q}{\partial x}|Q|^2 = 0. \tag{1.1}$$

Here, Q=Q(x,t) is representing the complex amplitude of a slowly varying optical field. The subscripts x and t indicate the spatial and temporal partial derivative respectively, and $|Q|^2Q_X$, $|Q|^2Q$, Q_{XX}, Q_{XXX} demonstrates the self-steepening, self-phase modulation, group velocity dispersion and third-order dispersion respectively [42]. The parameters β, λ, γ and δ in Eq (1.1) are the real constants that satisfies the relation $\lambda\beta = \delta\gamma$. To illustrate the generalization of the Hirota equation, some limiting cases will also be discussed:

(i) By setting $\lambda = \gamma = 0$, Eq (1.1) turns to the non-linear schrödinger equation [41].

(ii) By setting $\beta = \delta = 0$ with real Q, Eq (1.1) turns to the modified Korteweg de Vries equation [41].

The goal of this paper is to provide an intuition for the multi-wave non-linear Hirota equation with the fractional generalized approach. The algebraic extended process is adopted to get a series of solutions. We begin with a simple description and definition of the classical non-linear Hirota model. In Section 2, fractional operator's basic definitions and their properties are provided. In Section 3, fractional configuration of a non-linear multi-wave, the Hirota equation driven by three well-defined fractional-order operators covering the singular and non-singular kernel is represented. Section 4 provides the basic details about the extended algebraic method and its fractional implementation on the non-linear Hirota equation. Graphical analysis is presented and we concluded that the present fractional model gets the ordinary configuration that has a resemblance to the cubic Duffing equation. The solutions are also displaying the validity of the utilized technique with concern to yielding the analytical solutions of the non-linear equation.

2. Preliminaries

Basic notations and preliminaries are mentioned in subsections (2.1) and (2.2).

2.1. Modified Riemann-Liouville fractional order operator

Definition 2.1. *Consider $j : x \to j(x)$ is a continues function, but not exceptionally differentiable. The derivative comprises fractional-order α is explicated as in [43]:*

$${}^{RL}D_x^{\alpha} j(x) = \begin{cases} \frac{1}{\Gamma(\alpha)}\int_o^x (x-\zeta)^{-\alpha-1}(j(\zeta)-j(0))d\zeta, & \alpha < 0 \\ \frac{1}{\Gamma(\alpha)}\frac{d}{dx}\int_o^x (x-\zeta)^{-\alpha}(j(\zeta)-j(0))d\zeta, & 0 < \alpha < 1 \\ (j^n(\alpha))^{\alpha-n}, & n \le \alpha \le n+1, n \ge 1. \end{cases} \tag{2.1}$$

The characteristics of the modified Riemann-Liouville fractional derivative are [43]:

(1) ${}^{RL}D_x^{\alpha}(m(j(x)) + n(g(x))) = mD_x^{\alpha}(j(x)) + nD_x^{\alpha}(g(x))$;

(2) ${}^{RL}D_x^{\alpha}(k(j(x))) = kD_x^{\alpha}(j(x))$;

(3) ${}^{RL}D_x^{\alpha}x^{\xi} = \frac{\Gamma(1+\xi)}{\Gamma(1+\xi-\alpha)}x^{\xi-\alpha}$, $\xi \ge 0$.

2.2. β-fractional derivative

Definition 2.2. *β-fractional derivative is stated as [44]:*

$$ {}_0^B D_x^\alpha(j(x)) = \lim_{\varepsilon\to 0} \frac{j(x+\varepsilon(x+\frac{1}{\Gamma(\alpha)})) - j(x)}{\varepsilon}. \tag{2.2} $$

The characteristics of the fractional operator are [44]:

Theorem 2.1. *As* $0 < \alpha \leq 1,\ m, n, c \in \mathbb{R} and h(x), g(x)$ *are differentiable at* $t > o$, *so*

(1) ${}_0^B D_x^\alpha(c) = 0$;

(2) ${}_0^B D_x^\alpha(k(j(x))) = k\ {}_0^B D_x^\alpha(g(x))(j(x))$;

(3) ${}_0^B D_x^\alpha(m(j(x)) + n(g(x))) = m\ {}_0^B D_x^\alpha(j(x)) + n\ {}_0^B D_x^\alpha(g(x))$;

(4) ${}_0^B D_x^\alpha(j(x) * j(x)) = (g(x))\ {}_0^B D_x^\alpha(j(x)) * (j(x))\ {}_0^B D_x^\alpha(g(x))$;

(5) ${}_0^B D_x^\alpha(\frac{g(x)}{j(x)}) = \frac{(j(x))\ {}_0^B D_x^\alpha(g(x)) - (g(x))\ {}_0^B D_x^\alpha(j(x))}{(j(x))^2}$.

2.3. Atangana-Baleanu in Riemann-Liouville sense(ABR) fractional derivative

Definition 2.3. *Let* $F \in H^1(a, b),\ b > a$, *then Atangana-Baleanu fractional integral with* $0 < \alpha \leq 1$ *for the function* $F(t)$ *is [45]:*

$$ {}_0^{ABR} D_{a^+}^\alpha(h(t)) = \frac{ABR(\alpha)}{(1-\alpha)} \frac{d}{dt} \int_a^t h(\tau) E_\alpha(\frac{-\alpha(t-\tau)^\alpha}{1-\alpha}) d\tau, \tag{2.3} $$

where $ABR(\alpha)$ *is the normalized function such as* $ABR(1) = ABR(0) = 1$ *and* E_α *is Mittag-leffer function. Thus,*

$$ {}_0^{ABR} D_{a^+}^\alpha(h(t)) = \frac{ABR(\alpha)}{(1-\alpha)} \sum_{n=0}^{\infty} (\frac{-\alpha}{1-\alpha})^{nRL} I_a^{\alpha n} h(t). \tag{2.4} $$

3. Fractional forms of Eq (1.1)

The fractional arrangement of non-linear multi wave Hirota model by different fractional order derivative.

(1) Modified Riemann-Liouville fractional derivative is applying on Eq (1.1):

$$ i^{RL} D_t^\alpha Q + \beta^{RL} D_{xx}^{2\alpha} Q + \delta Q|Q|^2 + i\gamma^{RL} D_{xxx}^{3\alpha} Q + 3i\lambda^{RL} D_x^\alpha Q|Q|^2 = 0, \tag{3.1} $$

where ${}^{RL}D_x^\alpha$ and ${}^{RL}D_t^\alpha$ are modified RL fractional order operators w. r. t. to x and t.

(2) The β-fractional order operator on Eq (1.1):

$$ i^B D_t^\alpha Q + \beta^B D_{xx}^{2\alpha} Q + \delta Q|Q|^2 + i\gamma^B D_{xxx}^{3\alpha} Q + 3i\lambda^B D_x^\alpha Q|Q|^2 = 0, \tag{3.2} $$

where ${}_0^B D_t^\alpha$ and ${}_0^B D_x^\alpha$ are the β operators in sense of t and x.

(3) Atangana-Baleanu in sense of Riemann-Liouville (ABR) fractional order derivative applied on Eq (1.1):

$$ i^{ABR} D_t^\alpha Q + \beta Q_{xx} + \delta Q|Q|^2 + i\gamma Q_{xxx} + 3i\lambda Q_x|Q|^2 = 0, \tag{3.3} $$

where ${}_0^{ABR} D_t^\alpha$ is Atangana-Baleanu (AB) operators concerned to t.

3.1. Transformations concerned to fractional order derivative

Here, we will establish transformations concerned to operators for conversion of PDE to ODE:

$$Q = Q(x,t), \quad where \quad Q(x,t) = U(\epsilon)e^{i\theta(x,t)}. \tag{3.4}$$

We will build ϵ and θ according to fractional order operator.
(1) ϵ and θ for RL fractional order operator:

$$\begin{cases} \epsilon = e\frac{x^\alpha}{\alpha} - c\frac{t^\alpha}{\alpha}, \\ \theta = l\frac{x^\alpha}{\alpha} - m\frac{t^\alpha}{\alpha} + \gamma_o. \end{cases} \tag{3.5}$$

(2) ϵ and θ for β fractional operator:

$$\begin{cases} \epsilon = e\left(x + \frac{1}{\Gamma(\alpha)}\right)^\alpha - c\left(t + \frac{1}{\Gamma(\alpha)}\right)^\alpha, \\ \theta = l\left(x + \frac{1}{\Gamma(\alpha)}\right)^\alpha - m\left(t + \frac{1}{\Gamma(\alpha)}\right)^\alpha + \gamma_o. \end{cases} \tag{3.6}$$

(3) ϵ and θ for Atangana-Baleanu (AB) fractional order operator:

$$\begin{cases} \epsilon = ex - \frac{(1-\alpha)(ct^{-n\alpha})}{AB(\alpha)\sum_{n=0}^{\infty}\left(\frac{-\alpha}{1-\alpha}\right)\Gamma(1-\alpha n)}, \\ \theta = lx - \frac{(1-\alpha)(mt^{-n\alpha})}{AB(\alpha)\sum_{n=0}^{\infty}\left(\frac{-\alpha}{1-\alpha}\right)\Gamma(1-\alpha n)} + \gamma_o. \end{cases} \tag{3.7}$$

4. Multi-wave soliton solutions

4.1. Explanation of the scheme

New extended direct algebraic algorithm is detailed as [46].
Assume a PDE:

$$H(Q, Q_t, Q_x, Q_{tt}, Q_{xx}, ...) = 0. \tag{4.1}$$

PDE is transforming into ODE:

$$R(U, U', U'', ...) = 0, \tag{4.2}$$

with the aid of transformation:

$$Q(x,t) = U(\epsilon)e^{i\theta(x,t)}, \tag{4.3}$$

where $\epsilon = k_1x + k_2t$, $\theta = k_3x + k_4t + \gamma_0$ and prime in Eq (4.2) is representing the differentiation.
Let Eq (4.2) has solution in the following form:

$$U(\epsilon) = a_0 + \sum_{i=-j}^{j}\left[a_i(W(\epsilon))^i\right], \tag{4.4}$$

where

$$W'(\epsilon) = \ln(\rho)\left(\delta + \upsilon W(\epsilon) + \chi W^2(\epsilon)\right), \quad \rho \neq 0, 1, \tag{4.5}$$

χ, υ, and δ are real constants.
The solutions of Eq (4.5) concerning to parameters δ, υ and χ are:

Case 1. When $\upsilon^2 - 4\delta\chi < 0$ and $\chi \neq 0$,

$$W_1(\epsilon) = -\frac{\upsilon}{2\chi} + \frac{\sqrt{-\Xi}}{2\chi}\tan_\rho\left(\frac{\sqrt{-\Xi}}{2}\epsilon\right), \tag{4.6}$$

$$W_2(\epsilon) = -\frac{\upsilon}{2\chi} - \frac{\sqrt{-\Xi}}{2\chi}\cot_\rho\left(\frac{\sqrt{-\Xi}}{2}\epsilon\right), \tag{4.7}$$

$$W_3(\epsilon) = -\frac{\upsilon}{2\chi} + \frac{\sqrt{-\Xi}}{2\chi}\left(\tan_\rho\left(\sqrt{-\Xi}\epsilon\right) \pm \sqrt{mn}\sec_\rho\left(\sqrt{-\Xi}\epsilon\right)\right), \tag{4.8}$$

$$W_4(\epsilon) = -\frac{\upsilon}{2\chi} + \frac{\sqrt{-\Xi}}{2\chi}\left(\cot_\rho\left(\sqrt{-\Xi}\epsilon\right) \pm \sqrt{mn}\csc_\rho\left(\sqrt{-\Xi}\epsilon\right)\right), \tag{4.9}$$

$$W_5(\psi) = -\frac{\upsilon}{2\chi} + \frac{\sqrt{-\Xi}}{4\chi}\left(\tan_\rho\left(\frac{\sqrt{-\Xi}}{4}\epsilon\right) - \cot_\rho\left(\frac{\sqrt{-\Xi}}{4}\epsilon\right)\right). \tag{4.10}$$

Case 2. When $\upsilon^2 - 4\delta\chi > 0$ and $\chi \neq 0$,

$$W_6(\epsilon) = -\frac{\upsilon}{2\chi} - \frac{\sqrt{\Xi}}{2\chi}\tanh_\rho\left(\frac{\sqrt{\Xi}}{2}\epsilon\right), \tag{4.11}$$

$$W_7(\psi) = -\frac{\upsilon}{2\chi} - \frac{\sqrt{\Xi}}{2\chi}\coth_\rho\left(\frac{\sqrt{\Xi}}{2}\epsilon\right), \tag{4.12}$$

$$W_8(\epsilon) = -\frac{\upsilon}{2\chi} + \frac{\sqrt{\Xi}}{2\chi}\left(-\tanh_\rho\left(\sqrt{\Xi}\epsilon\right) \pm i\sqrt{mn}\ sech_\rho\left(\sqrt{\Xi}\epsilon\right)\right), \tag{4.13}$$

$$W_9(\epsilon) = -\frac{\upsilon}{2\chi} + \frac{\sqrt{\Xi}}{2\chi}\left(-\coth_\rho\left(\sqrt{\Xi}\epsilon\right) \pm \sqrt{mn}\,\mathrm{csch}_\rho\left(\sqrt{\Xi}\epsilon\right)\right), \tag{4.14}$$

$$W_{10}(\epsilon) = -\frac{\upsilon}{2\chi} - \frac{\sqrt{\Xi}}{4\chi}\left(\ tanh_\rho\left(\frac{\sqrt{\Xi}}{4}\epsilon\right) + \ coth_\rho\left(\frac{\sqrt{\Xi}}{4}\epsilon\right)\right). \tag{4.15}$$

Case 3. When $\delta\chi > 0$ and $\upsilon = 0$,

$$W_{11}(\psi) = \sqrt{\frac{\delta}{\chi}}\ tan_\rho\left(\sqrt{\delta\chi}\epsilon\right), \tag{4.16}$$

$$W_{12}(\epsilon) = -\sqrt{\frac{\delta}{\chi}}\ cot_\rho\left(\sqrt{\delta\chi}\epsilon\right), \tag{4.17}$$

$$W_{13}(\psi) = \sqrt{\frac{\delta}{\chi}}\left(\tan_\rho\left(2\sqrt{\delta\chi}\epsilon\right) \pm \sqrt{mn}\ sec_\rho\left(2\sqrt{\delta\chi}\epsilon\right)\right), \tag{4.18}$$

$$W_{14}(\epsilon) = \sqrt{\frac{\delta}{\chi}}\left(-\ cot_\rho\left(2\sqrt{\delta\chi}\epsilon\right) \pm \sqrt{mn}\csc_\rho\left(2\sqrt{\delta\chi}\epsilon\right)\right), \tag{4.19}$$

$$W_{15}(\epsilon) = \frac{1}{2}\sqrt{\frac{\delta}{\chi}}\left(\tan_\rho\left(\frac{\sqrt{\delta\chi}}{2}\epsilon\right) - \cot_\rho\left(\frac{\sqrt{\delta\chi}}{2}\epsilon\right)\right). \tag{4.20}$$

Case 4. When $\delta\chi < 0$ and $\upsilon = 0$,

$$W_{16}(\psi) = -\sqrt{-\frac{\delta}{\chi}}\tanh_\rho\left(\sqrt{-\delta\chi}\epsilon\right), \tag{4.21}$$

$$W_{17}(\epsilon) = -\sqrt{-\frac{\delta}{\chi}}\coth_\rho\left(\sqrt{-\delta\chi}\epsilon\right), \tag{4.22}$$

$$W_{18}(\epsilon) = \sqrt{-\frac{\delta}{\chi}}\left(-\tanh_\rho\left(2\sqrt{-\delta\chi}\epsilon\right) \pm i\sqrt{mn}\ sech_\rho\left(2\sqrt{-\delta\chi}\psi\right)\right), \tag{4.23}$$

$$W_{19}(\epsilon) = \sqrt{-\frac{\delta}{\chi}}\left(-\coth_\rho\left(2\sqrt{-\delta\chi}\epsilon\right) \pm \sqrt{mn}\ csch_\rho\left(2\sqrt{-\delta\chi}\epsilon\right)\right), \tag{4.24}$$

$$W_{20}(\epsilon) = -\frac{1}{2}\sqrt{-\frac{\delta}{\chi}}\left(\tanh_\rho\left(\frac{\sqrt{-\delta\chi}}{2}\epsilon\right) + \ coth_\rho\left(\frac{\sqrt{-\delta\chi}}{2}\epsilon\right)\right). \tag{4.25}$$

Case 5. When $\upsilon = 0$ and $\delta = \chi$,

$$W_{21}(\epsilon) = \tan_\rho(\delta\epsilon), \tag{4.26}$$

$$W_{22}(\epsilon) = -\cot_\rho(\delta\epsilon), \tag{4.27}$$

$$W_{23}(\epsilon) = \tan_\rho(2\delta\epsilon) \pm \sqrt{mn}\sec_\rho(2\delta\epsilon), \tag{4.28}$$

$$W_{24}(\epsilon) = -\cot_\rho(2\delta\epsilon) \pm \sqrt{mn}\csc_\rho(2\delta\epsilon), \tag{4.29}$$

$$W_{25}(\epsilon) = \frac{1}{2}\left(\tan_\rho\left(\frac{\delta}{2}\epsilon\right) - \cot_\rho\left(\frac{\delta}{2}\epsilon\right)\right). \tag{4.30}$$

Case 6. When $\upsilon = 0$ and $\chi = -\delta$,

$$W_{26}(\epsilon) = -\tanh_\rho(\delta\epsilon), \tag{4.31}$$

$$W_{27}(\epsilon) = -\coth_\rho(\delta\epsilon), \tag{4.32}$$

$$W_{28}(\epsilon) = -\tanh_\rho(2\delta\epsilon) \pm i\sqrt{mn}\ sech_\rho(2\delta\epsilon), \tag{4.33}$$

$$W_{29}(\epsilon) = -\coth_\rho(2\delta\epsilon) \pm \sqrt{mn}\ csch_\rho(2\delta\epsilon), \tag{4.34}$$

$$W_{30}(\epsilon) = -\frac{1}{2}\left(\tanh_\rho\left(\frac{\delta}{2}\epsilon\right) + \coth_\rho\left(\frac{\delta}{2}\epsilon\right)\right). \tag{4.35}$$

Case 7. When $\upsilon^2 = 4\delta\chi$,

$$W_{31}(\epsilon) = \frac{-2\delta(\upsilon\epsilon\ln\rho + 2)}{\upsilon^2\epsilon\ln\rho}. \tag{4.36}$$

Case 8. When $\delta = pq$, $\upsilon = p$, $\chi = 0$ and $(q \neq 0)$,

$$W_{32}(\epsilon) = \rho^{p\epsilon} - q. \tag{4.37}$$

Case 9. When $\upsilon = \chi = 0$,

$$W_{33}(\epsilon) = \delta\epsilon \ln \rho. \tag{4.38}$$

Case 10. When $\upsilon = \delta = 0$,

$$W_{34}(\epsilon) = \frac{-1}{\chi\epsilon \ln \rho}. \tag{4.39}$$

Case 11. When $\upsilon \neq 0$ and $\delta = 0$,

$$W_{35}(\epsilon) = -\frac{m\upsilon}{\chi\left(\cosh_\rho(\upsilon\psi) - \sinh_\rho(\upsilon\epsilon) + m\right)}, \tag{4.40}$$

$$W_{36}(\epsilon) = -\frac{\upsilon\left(\sinh_\rho(\upsilon\epsilon) + \cosh_\rho(\upsilon\epsilon)\right)}{\chi\left(\sinh_\rho(\upsilon\epsilon) + \cosh_\rho(\upsilon\epsilon) + n\right)}. \tag{4.41}$$

Case 12. When $\chi = pq$, $\upsilon = p$, $\delta = 0$ and $q \neq 0$,

$$W_{37}(\epsilon) = -\frac{m\rho^{p\epsilon}}{m - qn\rho^{p\epsilon}}, \tag{4.42}$$

$$\sinh_\rho(\epsilon) = \frac{m\rho^\epsilon - n\rho^{-\epsilon}}{2}, \quad \cosh_\rho(\epsilon) = \frac{m\rho^\epsilon + n\rho^{-\epsilon}}{2},$$

$$\tanh_\rho(\epsilon) = \frac{m\rho^\epsilon - n\rho^{-\epsilon}}{m\rho^\epsilon + n\rho^{-\epsilon}}, \quad \coth_\rho(\epsilon) = \frac{m\rho^\epsilon + n\rho^{-\epsilon}}{m\rho^\epsilon - n\rho^{-\epsilon}},$$

$$sech_\rho(\epsilon) = \frac{2}{m\rho^\epsilon + n\rho^{-\epsilon}}, \quad csch_\rho(\epsilon) = \frac{2}{m\rho^\epsilon - n\rho^{-\epsilon}},$$

$$sin_\rho(\epsilon) = \frac{m\rho^{i\epsilon} - n\rho^{-i\epsilon}}{2i}, \quad cos_\rho(\epsilon) = \frac{m\rho^{i\epsilon} + n\rho^{-i\epsilon}}{2},$$

$$\tan_\rho(\epsilon) = -i\frac{m\rho^{i\epsilon} - n\rho^{-i\epsilon}}{m\rho^{i\epsilon} + n\rho^{-i\epsilon}}, \quad \cot_\rho(\epsilon) = i\frac{m\rho^{i\epsilon} + n\rho^{-i\epsilon}}{m\rho^{i\epsilon} - n\rho^{-i\epsilon}},$$

$$\sec_\rho(\epsilon) = \frac{2}{m\rho^\epsilon + n\rho^{-\epsilon}}, \quad \csc_\rho(\epsilon) = \frac{2i}{m\rho^\epsilon - n\rho^{-\epsilon}}.$$

The deformation parameters m and n are arbitrary constants greater than zero.

4.2. Application to Eq (4.1)

Applying the transformations Eqs (3.5)–(3.7) on the Eqs (3.1)–(3.3) respectively. The real and imaginary parts of the obtained ordinary differential equation are respectively:

$$e^2(\beta - 3\gamma l)U''(\epsilon) + (m + \gamma l^3 - l^2\beta)U(\epsilon) + (\delta - 3\lambda l)U^3(\epsilon) = 0, \tag{4.43}$$

$$\left(c + 3\beta el - 3\gamma el^2\right)U'(\epsilon) + 3\lambda eU^2(\epsilon)U'(\epsilon) + \gamma e^3U'''(\epsilon) = 0, \tag{4.44}$$

where $c = 3\gamma el^2 - 2\beta le$. The homogeneous balancing constant N=1 of Eq (4.43). Therefore, the solution can be written in the form

$$U(\epsilon) = a_0 + a_1(W(\epsilon)), \tag{4.45}$$

where

$$W'(\epsilon) = \ln(\rho)\left(\delta + \upsilon Q(\epsilon) + \chi Q^2(\psi)\right), \quad \rho \neq 0, 1. \tag{4.46}$$

By using Eq (4.45) into Eq (4.43) and equating the coefficients of different powers of $W(\epsilon)$, we will obtain a system of algebraic equations which can be solved with the help of Mathematica software:

$$\left[a_0 = \pm\frac{\upsilon e\sqrt{\beta - 3l\gamma}}{\sqrt{6l\lambda - 2\delta}}\log[\rho], \;\; a_1 = \pm\frac{2\chi e\sqrt{\beta - 3l\gamma}}{\sqrt{6l\lambda - 2\delta}}\log[\rho], \;\; m = l^2(\beta - l\gamma) + \frac{1}{2}e^2(\beta - 3\gamma l)\Xi\log[\rho]^2\right]. \tag{4.47}$$

We get the general solution by substituting Eq (4.47) into Eq (4.45):

$$Q(x,t) = (\upsilon\Omega + 2\chi\Omega(W_i(\epsilon))) \times e^{i\theta(x,t)}. \tag{4.48}$$

Here, $\Omega = \pm\frac{e\sqrt{\beta-3l\gamma}}{\sqrt{6l\lambda-2\delta}}\log[\rho]$ and $\Xi = \upsilon^2 - 4\delta\chi$. Many different solutions can be generated by taking W_i from the Eqs (4.6)–(4.42).

Case 1. When $\upsilon^2 - 4\delta\chi < 0$ and $\chi \neq 0$,

$$Q_1(x,t) = \Omega\sqrt{-\Xi}\tan_\rho\left(\frac{\sqrt{-\Xi}}{2}\epsilon\right) \times e^{i\theta(x,t)}, \tag{4.49}$$

$$Q_2(x,t) = -\Omega\sqrt{-\Xi}\cot_\rho\left(\frac{\sqrt{-\Xi}}{2}\epsilon\right) \times e^{i\theta(x,t)}, \tag{4.50}$$

$$Q_3(x,t) = \Omega\sqrt{-\Xi}\left(\tan_\rho\left(\sqrt{-\Xi}\epsilon\right) \pm \sqrt{mn}\sec_\rho\left(\sqrt{-\Xi}\epsilon\right)\right) \times e^{i\theta(x,t)}, \tag{4.51}$$

$$Q_4(x,t) = \Omega\sqrt{-\Xi}\left(\cot_\rho\left(\sqrt{-\Xi}\epsilon\right) \pm \sqrt{mn}\csc_\rho\left(\sqrt{-\Xi}\epsilon\right)\right) \times e^{i\theta(x,t)}, \tag{4.52}$$

$$Q_5(x,t) = \frac{\Omega\sqrt{-\Xi}}{2}\left(\tan_\rho\left(\frac{\sqrt{-\Xi}}{4}\epsilon\right) - \cot_\rho\left(\frac{\sqrt{-\Xi}}{4}\epsilon\right)\right) \times e^{i\theta(x,t)}. \tag{4.53}$$

Case 2. When $\upsilon^2 - 4\delta\chi > 0$ and $\chi \neq 0$,

$$Q_6(x,t) = \Omega\sqrt{-\Xi}\tanh_\rho\left(\frac{\sqrt{-\Xi}}{2}\epsilon\right) \times e^{i\theta(x,t)}, \tag{4.54}$$

$$Q_7(x,t) = -\Omega\sqrt{-\Xi}\coth_\rho\left(\frac{\sqrt{-\Xi}}{2}\epsilon\right) \times e^{i\theta(x,t)}, \tag{4.55}$$

$$Q_8(x,t) = \Omega\sqrt{-\Xi}\left(\tanh_\rho\left(\sqrt{-\Xi}\epsilon\right) \pm \iota\sqrt{mn}\,\mathrm{sech}_\rho\left(\sqrt{-\Xi}\epsilon\right)\right) \times e^{i\theta(x,t)}, \tag{4.56}$$

$$Q_9(x,t) = \Omega\sqrt{-\Xi}\left(\coth_\rho\left(\sqrt{-\Xi}\epsilon\right) \pm \sqrt{mn}_\rho\left(\sqrt{-\Xi}\epsilon\right)\right) \times e^{i\theta(x,t)}, \tag{4.57}$$

$$Q_{10}(x,t) = -\frac{\Omega\sqrt{\Xi}}{4\chi}\left(\tanh_\rho\left(\frac{\sqrt{\Xi}}{4}\epsilon\right) + \coth_\rho\left(\frac{\sqrt{\Xi}}{4}\epsilon\right)\right) \times e^{i\theta(x,t)}. \tag{4.58}$$

Case 3. When $\delta\chi > 0$ and $\upsilon = 0$,

$$Q_{11}(x,t) = 2\Omega\sqrt{\delta\chi}\,tan_\rho\left(\sqrt{\delta\chi}\epsilon\right) \times e^{i\theta(x,t)}, \tag{4.59}$$

$$Q_{12}(x,t) = -2\chi\left(\sqrt{\delta\chi}\; cot_\rho\left(\sqrt{\delta\chi}\epsilon\right)\right)\times e^{i\theta(x,t)}, \tag{4.60}$$

$$Q_{13}(x,t) = 2\Omega\left(\sqrt{\delta\chi}\left(\tan_\rho\left(2\sqrt{\delta\chi}\epsilon\right)\pm\sqrt{mn}\; sec_\rho\left(2\sqrt{\delta\chi}\epsilon\right)\right)\right)\times e^{i\theta(x,t)}, \tag{4.61}$$

$$Q_{14}(x,t) = 2\Omega\left(\sqrt{\delta\chi}\left(-\,cot_\rho\left(2\sqrt{\delta\chi}\epsilon\right)\pm\sqrt{mn}\; csc_\rho\left(2\sqrt{\delta\chi}\epsilon\right)\right)\right)\times e^{i\theta(x,t)}, \tag{4.62}$$

$$Q_{15}(x,t) = \Omega\left(\sqrt{\delta\chi}\left(\tan_\rho\left(\frac{\sqrt{\delta\chi}}{2}\epsilon\right)-\cot_\rho\left(\frac{\sqrt{\delta\chi}}{2}\epsilon\right)\right)\right)\times e^{i\theta(x,t)}. \tag{4.63}$$

Case 4. When $\delta\chi < 0$ and $\upsilon = 0$,

$$Q_{16}(x,t) = -2\Omega\left(\sqrt{-\delta\chi}\tanh_\rho\left(\sqrt{-\delta\chi}\epsilon\right)\right)\times e^{i\theta(x,t)}, \tag{4.64}$$

$$Q_{17}(x,t) = -2\Omega\left(\sqrt{-\delta\chi}\coth_\rho\left(\sqrt{-\delta\chi}\epsilon\right)\right)\times e^{i\theta(x,t)}, \tag{4.65}$$

$$Q_{18}(x,t) = 2\Omega\left(\sqrt{-\delta\chi}\left(-\tanh_\rho\left(2\sqrt{-\delta\chi}\epsilon\right)\pm i\sqrt{mn}\; sech_\rho\left(2\sqrt{-\delta\chi}\psi\right)\right)\right)\times e^{i\theta(x,t)}, \tag{4.66}$$

$$Q_{19}(x,t) = 2\Omega\left(\sqrt{-\delta\chi}\left(-\coth_\rho\left(2\sqrt{-\delta\chi}\epsilon\right)\pm\sqrt{mn}\,\mathrm{csch}_\rho\left(2\sqrt{-\delta\chi}\epsilon\right)\right)\right)\times e^{i\theta(x,t)}, \tag{4.67}$$

$$Q_{20}(x,t) = -\Omega\left(\sqrt{-\delta\chi}\left(\tanh_\rho\left(\frac{\sqrt{-\delta\chi}}{2}\epsilon\right)+\; coth_\rho\left(\frac{\sqrt{-\delta\chi}}{2}\epsilon\right)\right)\right)\times e^{i\theta(x,t)}. \tag{4.68}$$

Case 5. When $\upsilon = 0$ and $\delta = \chi$,

$$Q_{21}(x,t) = 2\chi\Omega\left(\tan_\rho(\chi\epsilon)\right)\times e^{i\theta(x,t)}, \tag{4.69}$$

$$Q_{22}(x,t) = 2\chi\Omega\left(-\cot_\rho(\chi\epsilon)\right)\times e^{i\theta(x,t)}, \tag{4.70}$$

$$Q_{23}(x,t) = 2\chi\Omega\left(\tan_\rho(2\chi\epsilon)\pm\sqrt{mn}\sec_\rho(2\chi\epsilon)\right)\times e^{i\theta(x,t)}, \tag{4.71}$$

$$Q_{24}(x,t) = 2\chi\Omega\left(-\cot_\rho(2\chi\epsilon)\pm\sqrt{mn}\csc_\rho(2\chi\epsilon)\right)\times e^{i\theta(x,t)}, \tag{4.72}$$

$$Q_{25}(x,t) = \chi\Omega\left(\left(\tan_\rho\left(\frac{\chi}{2}\epsilon\right)-\cot_\rho\left(\frac{\chi}{2}\epsilon\right)\right)\right)\times e^{i\theta(x,t)}. \tag{4.73}$$

Case 6. When $\upsilon = 0$ and $\delta = -\chi$,

$$Q_{26}(x,t) = 2\chi\Omega\left(-\tanh_\rho(-\chi\epsilon)\right)\times e^{i\theta(x,t)}, \tag{4.74}$$

$$Q_{27}(x,t) = 2\chi\Omega\left(-\coth_\rho(-\chi\epsilon)\right)\times e^{i\theta(x,t)}, \tag{4.75}$$

$$Q_{28}(x,t) = 2\chi\Omega\left(-\tanh_\rho(-2\chi\epsilon)\pm i\sqrt{mn}\; sech_\rho(-2\chi\epsilon)\right)\times e^{i\theta(x,t)}, \tag{4.76}$$

$$Q_{29}(x,t) = 2\chi\Omega\left(-\coth_\rho(-2\chi\epsilon)\pm\sqrt{mn}\; csch_\rho(-2\chi\epsilon)\right)\times e^{i\theta(x,t)}, \tag{4.77}$$

$$Q_{30}(x,t) = -\chi\Omega\left(\left(\tanh_\rho\left(\frac{-\chi}{2}\epsilon\right)+\coth_\rho\left(\frac{-\chi}{2}\epsilon\right)\right)\right)\times e^{i\theta(x,t)}. \tag{4.78}$$

Case 7. When $\upsilon^2 = \sqrt{4\delta\chi}$,

$$Q_{31}(x,t) = \Omega\sqrt{4\delta\chi}+\Omega\left(\frac{-(\sqrt{4\delta\chi}\epsilon\ln\rho+2)}{\epsilon\ln\rho}\right)\times e^{i\theta(x,t)}. \tag{4.79}$$

Case 8. When $\delta = pq$, $q \neq 0$, $\upsilon = p$ and $\chi = 0$,

$$Q_{32}(x,t) = Constant\ solution. \tag{4.80}$$

Case 9. When $\upsilon = 0$ and $\chi = 0$,

$$Q_{33}(x,t) = 0. \tag{4.81}$$

Case 10. When $\upsilon = 0$ and $\delta = 0$,

$$Q_{34}(x,t) = -2\Omega\left(\frac{1}{\epsilon ln[\rho]}\right) \times e^{i\theta(x,t)}. \tag{4.82}$$

Case 11. When $\upsilon \neq 0$ and $\delta = 0$,

$$Q_{35}(\epsilon) = \upsilon\Omega - 2\Omega\left(-\frac{m\upsilon}{\left(\cosh_\rho(\upsilon\psi) - \sinh_\rho(\upsilon\epsilon) + m\right)}\right) \times e^{i\theta(x,t)}, \tag{4.83}$$

$$Q_{36}(\epsilon) = \upsilon\Omega - 2\Omega\left(\frac{\upsilon\left(\sinh_\rho(\upsilon\epsilon) + \cosh_\rho(\upsilon\epsilon)\right)}{\left(\sinh_\rho(\upsilon\epsilon) + \cosh_\rho(\upsilon\epsilon) + n\right)}\right) \times e^{i\theta(x,t)}. \tag{4.84}$$

Case 12. When $\chi = pq$, $\upsilon = p$, $q \neq 0$ and $\delta = 0$,

$$Q_{37}(\epsilon) = \upsilon\Omega - 2\chi\Omega\left(\frac{m\rho^{p\epsilon}}{m - qn\rho^{p\epsilon}}\right) \times e^{i\theta(x,t)}. \tag{4.85}$$

Adopt the ϵ and θ as per concerning fractional derivative from Eqs (3.5)–(3.7) corresponding to Riemann-Liouvilla, β and Atangana-Baleanue operators respectively.

5. Graphical analysis

Figure 1 is providing 2D and 3D graphical description of complex amplitude of waves for the solution $Q_1(x,t)$ with the parametric values are $\rho = 0.5$, $\gamma = 1$, $\gamma_0 = 1$, $\delta = 1$, $\lambda = 1$, $\beta = 1$, $l = 0.4$, $e = 0.3$, $\upsilon = 1$, $\chi = 1$ and $\delta = 1$ by utilizing the RL, β and AB fractional operator for $\alpha = 0.1$. Figure (1a)–(1c) is 3D presentation of complex amplitude that is displaying the bright-dark, bright and bright periodic singular behavior with the RL, β and AB fractional order derivatives respectively. Figure (1d) is made to portray 2D graphical comparison of the fractional operators used to attain our results.

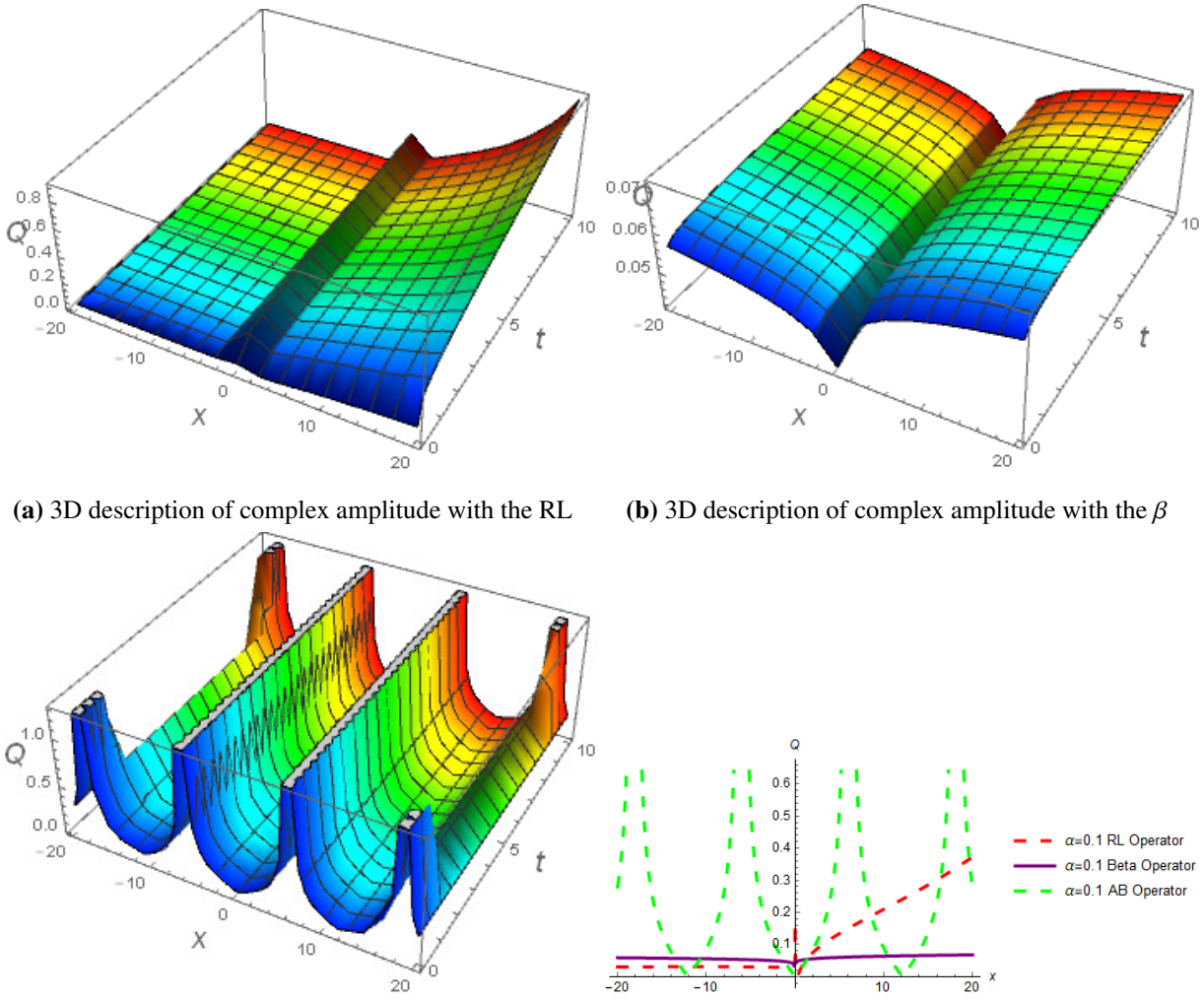

(a) 3D description of complex amplitude with the RL **(b)** 3D description of complex amplitude with the β

(c) 3D description of complex amplitude with AB **(d)** 2D graphical comparison of the operators

Figure 1. Three dimensional graphical explanation for $Q_1(x,t)$ at the $\alpha = 0.1$.

Figure 2 is providing 2D and 3D graphical description of complex amplitude of waves for the solution $Q_1(x,t)$ with the parametric values are $\rho = 0.5$, $\gamma = 1$, $\gamma_0 = 1$, $\delta = 1$, $\lambda = 1$, $\beta = 1$, $l = 0.4$, $e = 0.3$, $\upsilon = 1$, $\chi = 1$ and $\delta = 1$ by utilizing the RL, β, and AB fractional operator at the $\alpha = 0.5$. Figure (2a)–(2c) is 3D presentation of complex amplitude that is displaying the bright singular, bright and bright-singular periodic behavior with the RL, β and AB fractional derivative respectively. Figure (2d) is displaying 2D graphical comparison of the utilized fractional operators.

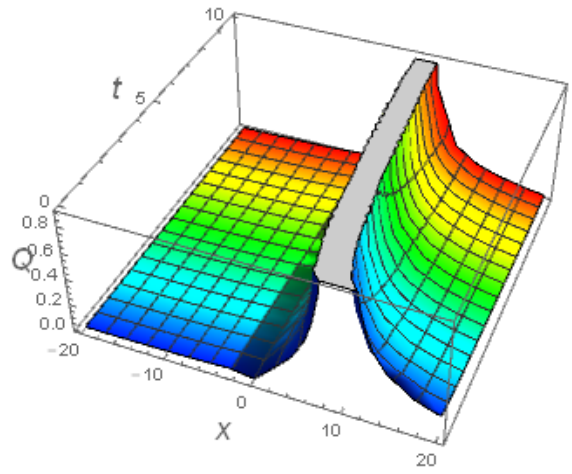

(a) 3D description of complex amplitude with the RL

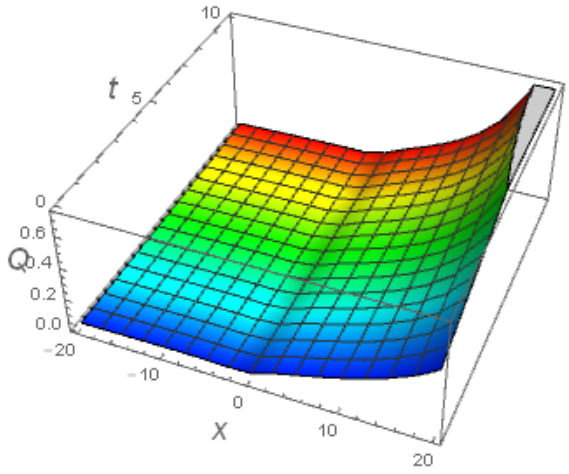

(b) 3D description of complex amplitude with the β

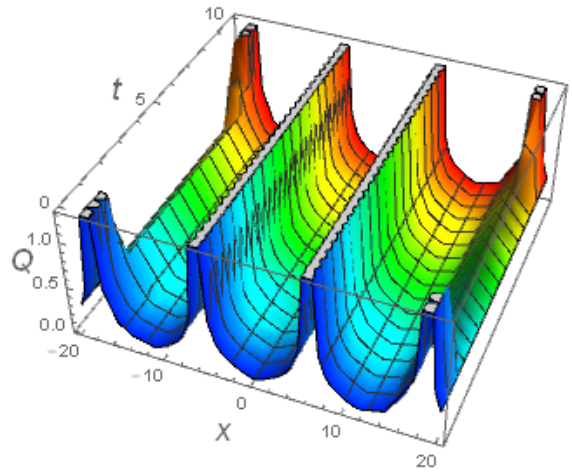

(c) 3D description of complex amplitude with the AB

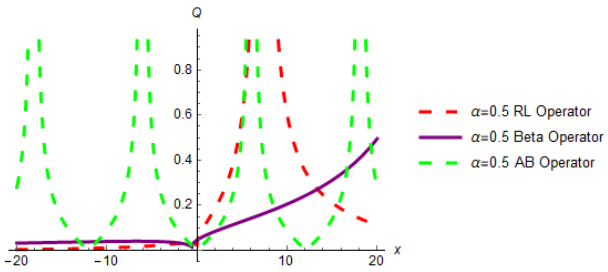

(d) 2D graphical comparison of the operators

Figure 2. Three dimensional graphical explanation for $Q_1(x,t)$ at the $\alpha = 0.5$.

Figure 3 is providing description of complex amplitude of waves for the solution $Q_1(x,t)$ with the parametric values are $\rho = 0.5,\ \gamma = 1,\ \gamma_0 = 1,\ \delta = 1,\ \lambda = 1,\ \beta = 1,\ l = 0.4,\ e = 0.3,\ \upsilon = 1,\ \chi = 1$ and $\delta = 1$ by utilizing the RL, β and AB fractional operator at the $\alpha = 0.9$. Figure (3a)–(3c) is 3D presentation of complex amplitude that is displaying the bright-singular, bright-singular, and bright periodic singular behavior with the RL, β and AB fractional derivative respectively. Figure (3d) is displaying 2D graphical comparison of the utilized fractional operators.

Remark 5.1. *It is observed that as we increase the fractional-order towards the classical order operators are trying to get a similar pattern.*

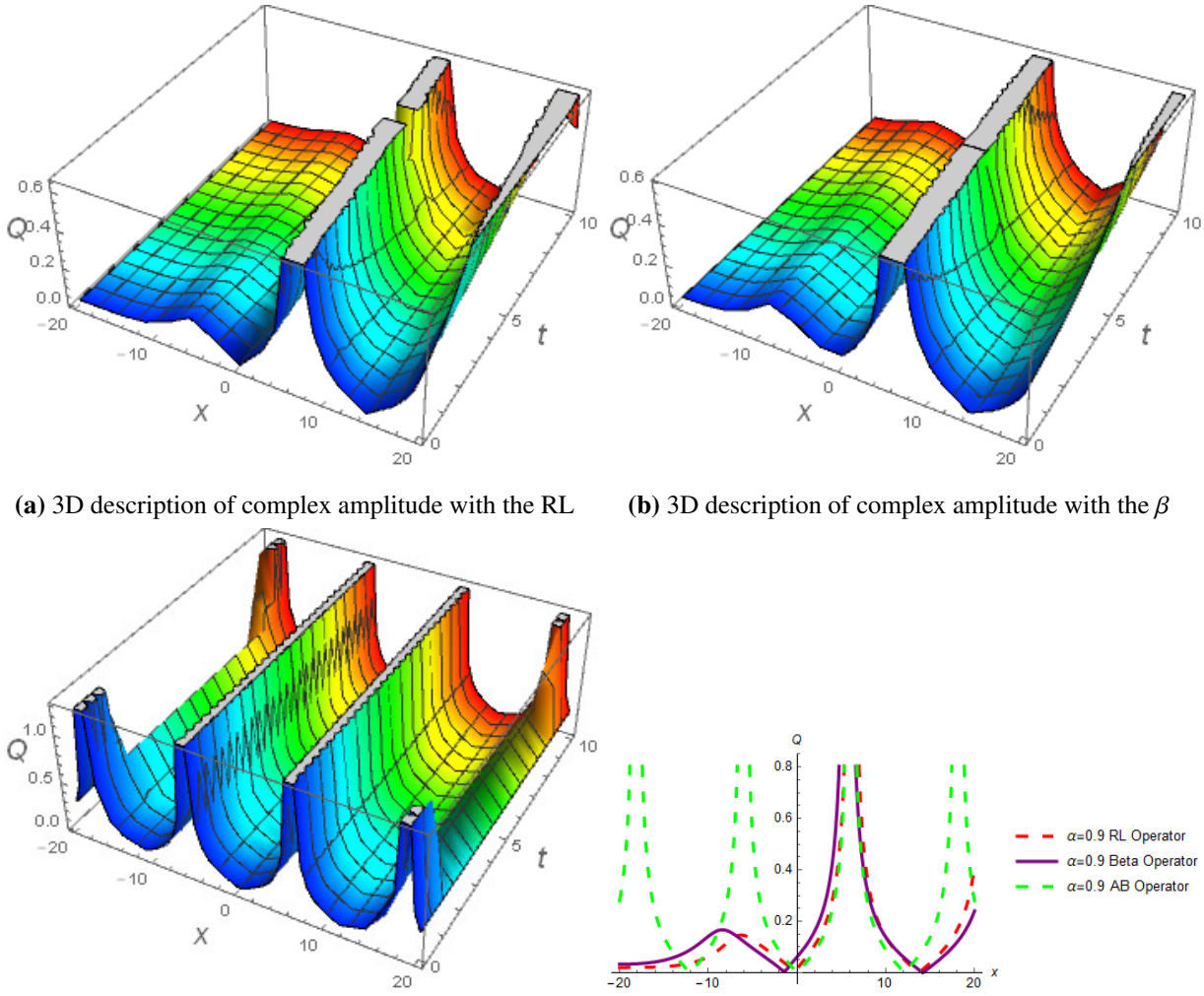

(a) 3D description of complex amplitude with the RL

(b) 3D description of complex amplitude with the β

(c) 3D description of complex amplitude with the AB

(d) 2D graphical comparison of the operators

Figure 3. Three dimensional graphical explanation for $Q_1(x,t)$ at the $\alpha = 0.9$.

Figure 4 is depicting the 2D graphical comparison of utilized operators and influence of fractional order for the solution $Q_1(x,t)$ with the parametric values are $\rho = 0.5,\ \gamma = 1, \gamma_0 = 1, \delta = 1, \lambda = 1, \beta = 1,$ $l = 0.4,\ e = 0.3,\ \upsilon = 1,\ \chi = 1$ and $\delta = 1$ by utilizing the RL, β and AB fractional operator. Figure (4a) is comparison of fractional and classical results. Figure (4b)–(4d) are showing the difference due to variation of fractional order for the RL, β and AB operator.

Remark 5.2. *It is investigated that the behavior with RL and β-fractional derivative is showing fluctuations due to variance of fractional order but AB operator is same throughout.*

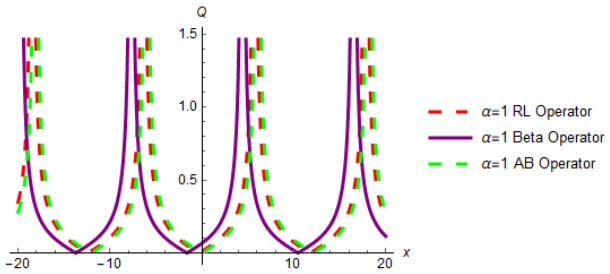

(a) 2D comparison at classic order

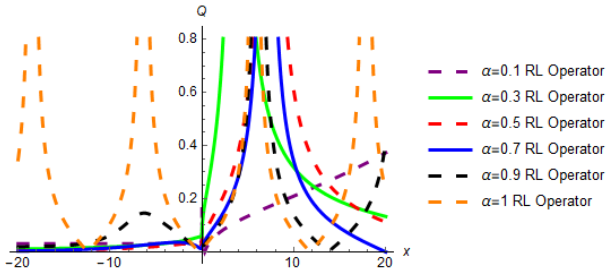

(b) 2D graphical impact of α on RL

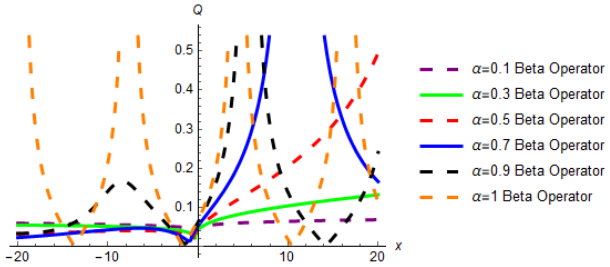

(c) 2D graphical impact of α on β

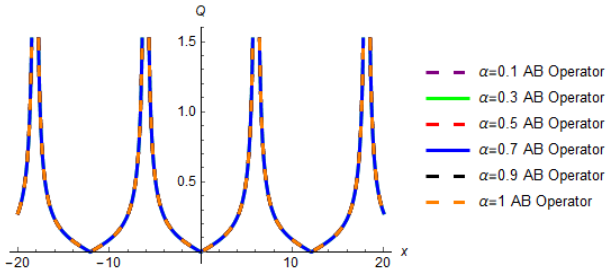

(d) 2D graphical impact of α on AB

Figure 4. Two dimensional graphical explanation for $Q_1(x,t)$ at classic order and variance of fractional order.

Figure 5 is providing 2D and 3D graphical description of complex amplitude of waves for the solution $Q_{35}(x,t)$ with the parametric values are $\rho = 0.5$, $\gamma = 1$, $\gamma_0 = 1$, $\delta = 1$, $\lambda = 1$, $\beta = 1$, $l = 0.4$, $e = 0.3$, $\upsilon = 1$ and $\delta = 0$ by utilizing the RL, β and AB fractional operator at the $\alpha = 0.1$. Figure (5a)–(5c) is 3D presentation of complex amplitude that is displaying the dark, bright and bright-dark behavior with RL, β and AB fractional derivative respectively. Figure (5d) is displaying 2D graphical comparison of the utilized fractional operators.

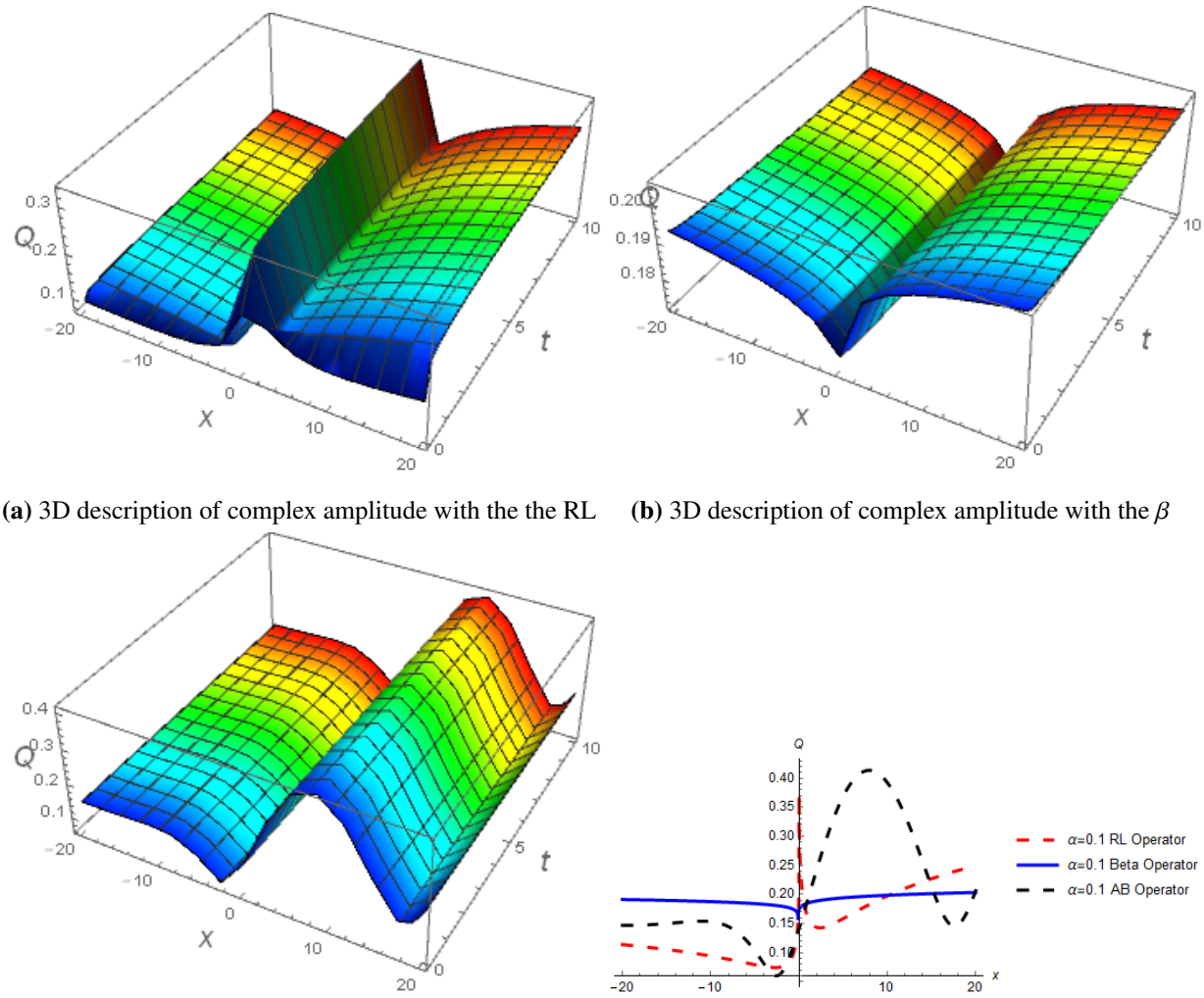

(a) 3D description of complex amplitude with the the RL **(b)** 3D description of complex amplitude with the β

(c) 3D description of complex amplitude with the AB **(d)** 2D graphical comparison of the operators

Figure 5. Three dimensional graphical explanation for $Q_{35}(x,t)$ at the $\alpha = 0.1$.

Figure 6 is providing 2D and 3D graphical description of complex amplitude of waves for the solution $Q_{35}(x,t)$ with the parametric values are $\rho = 0.5$, $\gamma = 1$, $\gamma_0 = 1$, $\delta = 1$, $\lambda = 1$, $\beta = 1$, $l = 0.4$, $e = 0.3$, $\upsilon = 1$ and $\delta = 0$ by utilizing the RL, β and AB fractional operator at the $\alpha = 0.5$. Figure (6a)–(6c) are 3D presentation of complex amplitude that is displaying the dark, bright and bright-dark behavior with the RL, β and AB fractional derivative. Figure (6d) is displaying 2D graphical comparison of the utilized fractional operators.

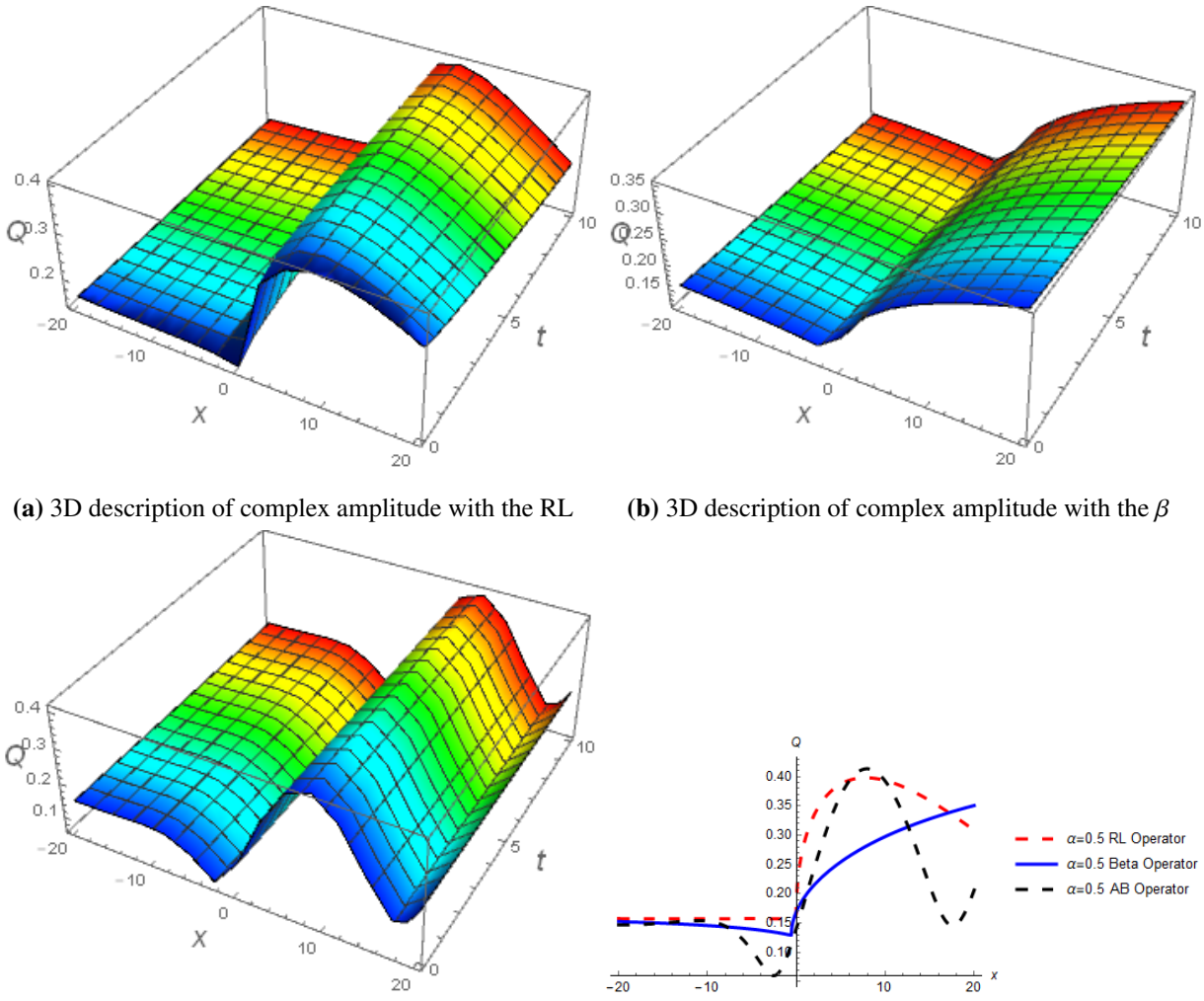

(a) 3D description of complex amplitude with the RL

(b) 3D description of complex amplitude with the β

(c) 3D description of complex amplitude with the AB

(d) 2D graphical comparison of the operators

Figure 6. Three dimensional graphical explanation for $Q_{35}(x,t)$ at the $\alpha = 0.5$.

Figure 7 is providing 2D and 3D graphical description of complex amplitude of waves for the solution $Q_{35}(x,t)$ with the parametric values are $\rho = 0.5$, $\gamma = 1$, $\gamma_0 = 1$, $\delta = 1$, $\lambda = 1$, $\beta = 1$, $l = 0.4$, $e = 0.3$, $\upsilon = 1$ and $\delta = 0$ by utilizing the RL, β and AB fractional operator at the $\alpha = 0.9$. Figure (7a)–(7c) is 3D presentation of complex amplitude that is displaying the bright-dark, bright-dark and bright-dark behavior with RL, β and AB fractional derivative respectively. Figure (7d) is displaying 2D graphical comparison of the utilized fractional operators.

Remark 5.3. *It is observed that as we increase the fractional order towards the classical order operators are trying to get similar pattern.*

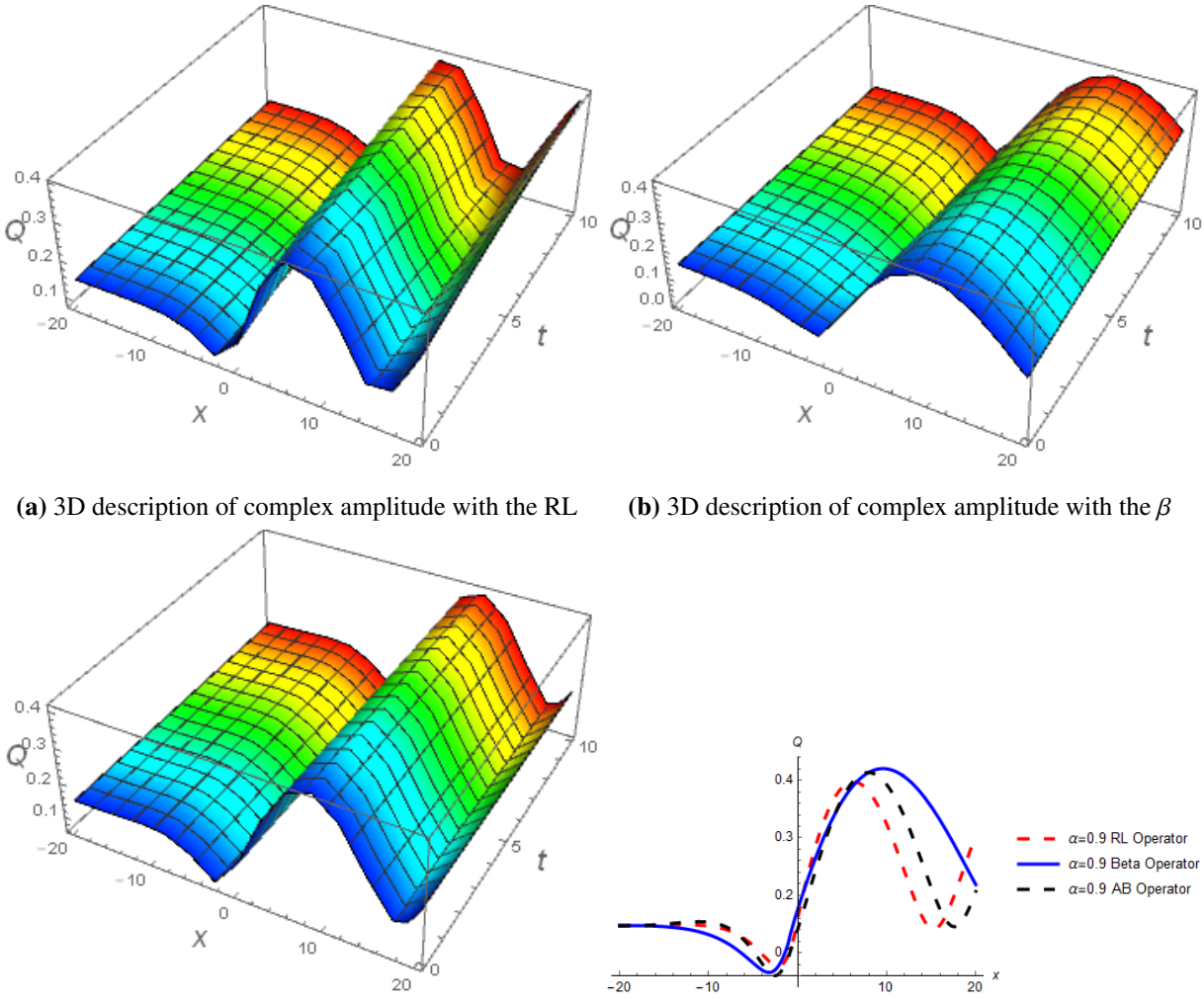

(a) 3D description of complex amplitude with the RL

(b) 3D description of complex amplitude with the β

(c) 3D description of complex amplitude with the AB

(d) 2D graphical comparison of the operators

Figure 7. Three dimensional graphical explanation for $Q_{35}(x,t)$ at the $\alpha = 0.9$.

Figure 8 is depicting the 2D graphical comparison of utilized operators and influence of fractional operator for the solution $Q_{35}(x,t)$ with the parametric values are $\rho = 0.5$, $\gamma = 1$, $\gamma_0 = 1$, $\delta = 1$, $\lambda = 1$, $\beta = 1$, $l = 0.4$, $e = 0.3$, $\upsilon = 1$ and $\delta = 0$ by utilizing the RL, β and AB fractional operator. Figure (8a) provides a comparison of fractional and classical results. Figure (8b)–(8d) are showing the difference due to variation of fractional order for the RL, β and AB operator.

Remark 5.4. *It is investigated that the behavior with RL and β-fractional derivative is showing fluctuations due to the variance of fractional order but the AB operator is the same throughout.*

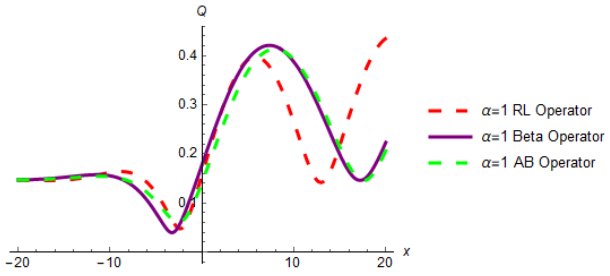

(a) 2D comparison at classic order

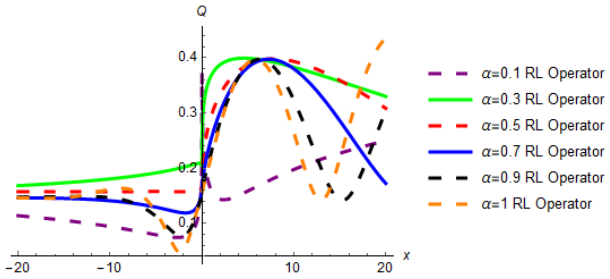

(b) 2D graphical impact of fractional order on the RL

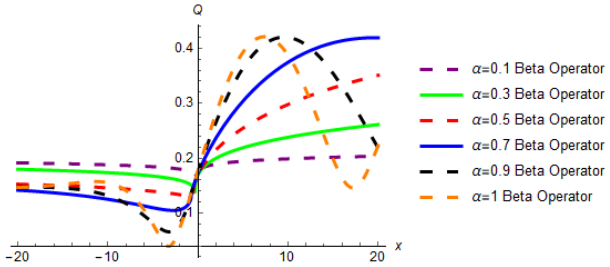

(c) 2D graphical impact of fractional order on the β

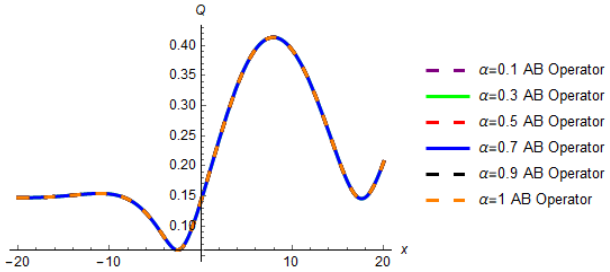

(d) 2D graphical impact of fractional order on the AB

Figure 8. Two dimensional graphical explanation for $Q_{35}(x,t)$ at classic order and variance of fractional order.

6. Conclusions

The present study has developed a multi-wave non-linear fractional Hirota model from the classical non-linear Hirota equation with the help of three different fractional definitions namely as Riemann-Liouville fractional order derivative, β-fractional operator, and Atangana-Baleanu in sense of Riemann-Liouville derivative. This fractional model gets the ordinary configuration that has a resemblance to the cubic Duffing equation. The extended direct algebraic method has been deployed with success to extract the exact traveling wave solutions. The obtained results carry some new features specifically, trigonometric, exponential, rational, and hyperbolic functions that delineate an interesting pattern of waves in the non-linear optical field. The important outcomes are listed below:

- On the same value of fractional order, Riemann-Liouville derivative predicted dark-singular soliton, the β-fractional operator exhibited dark soliton, while the Atangana-Baleanu operator delineated dark-singular-periodic soliton.
- The Atangan-Baleanu fractional operator is more reliable operator as compared to Riemann-Liouville and β-fractional operator.
- The Atangana-Baleanu derivative is also more consistent than Riemann-Liouville and β differential operator.

To interpret the graphic phenomenon, 2D and 3D plots are plotted by holding suitable values of the involved parameters. The extracted solutions are also evidence of method liability and a remarkable role in treating the non-linear complex models.

Acknowledgments

The authors are greatly thankful to the University of Management and Technology Lahore, Pakistan for facilitating and supporting that research work.

Conflict of interest

The authors state no conflicts of interest.

References

1. K. S. Miller, B. Ross, *An introduction to the fractional calculus and fractional differential equations*, New York: Wiley, 1993.
2. A. A. Kilbas, H. M. Srivastava, J. J. Trujillo, *Theory and applications of fractional differential equations*, Amsterdam: Elsevier, 2006.
3. I. Podlubny, *Fractional diferential equations*, California: Academic Press, 1999.
4. C. Park, M. M. A. Khater, A. H. Abdel-Aty, R. A. M. Attia, H. Rezazadeh, A. M. Zidan, et al., Dynamical analysis of the nonlinear complex fractional emerging telecommunication model with higher-order dispersive cubic-quintic, *Alex. Eng. J.*, **59** (2020), 1425–1433. https://doi.org/10.1016/j.aej.2020.03.046

5. K. U. Tariq, M. Younis, H. Rezazadeh, S. T. R. Rizvi, M. S. Osman, Optical solitons with quadratic-cubic nonlinearity and fractional temporal evolution, *Mod. Phys. Lett. B*, **32** (2018), 1–13. https://doi.org/10.1142/S0217984918503177
6. H. Rezazadeh, H. Aminikhah, A. R. Sheikhani, A new algorithm for solving of fractional differential equation with time delay, In: *The 10th seminar on differential equations and dynamic systems*, 2013, 194–197.
7. H. H. Asada, F. E. Sotiropoulos, Dual faceted linearization of nonlinear dynamical systems based on physical modeling theory, *J. Dyn. Sys. Meas. Control*, **141** (2019), 1–11. https://doi.org/10.1115/1.4041448
8. C. Gérard, C. D. Jäkel, Thermal quantum fields without cut-offs in 1+1 space-time dimensions, *Rev. Math. Phy.*, **17** (2005), 113–173. https://doi.org/10.1142/S0129055X05002303
9. A. Atangana, S. I. Araz, Atangana-Seda numerical scheme for Labyrinth attractor with new differential and integral operators, *Fractals*, **28** (2020), 1–18. https://doi.org/10.1142/S0218348X20400447
10. A. Atangana, S. I. Araz, Mathematical model of COVID-19 spread in Turkey and South Africa: Theory, methods, and applications, *Adv. Differ. Equ.*, **2020** (2020), 1–89. https://doi.org/10.1186/s13662-020-03095-w
11. A. Atangana, S. I. Araz, Modeling and forecasting the spread of COVID-19 with stochastic and deterministic approaches: Africa and Europe, *Adv. Differ. Equ.*, **2021** (2021), 1–107. https://doi.org/10.1186/s13662-021-03213-2
12. A. Atangana, S. I. Araz, Nonlinear equations with global differential and integral operators: Existence, uniqueness with application to epidemiology, *Results Phys.*, **20** (2020), 103593. https://doi.org/10.1016/j.rinp.2020.103593
13. M. Mirzazadeh, Analytical study of solitons to nonlinear time fractional parabolic equations, *Nonlinear Dyn.*, **85** (2016), 2569–2576. https://doi.org/10.1007/s11071-016-2845-7
14. E. Tala-Tebue, Z. I. Djoufack, A. Djimeli-Tsajio, A. Kenfack-Jiotsa, Solitons and other solutions of the nonlinear fractional Zoomeron equation, *Chinese J. Phys.*, **56** (2018), 1232–1246. https://doi.org/10.1016/j.cjph.2018.04.017
15. E. Tala-Tebue, C. Tetchoka-Manemo, H. Rezazadeh, A. Bekir, Y. M. Chu, Optical solutions of the (2+1)-dimensional hyperbolic nonlinear Schrödinger equation using two different methods, *Results Phys.*, **19** (2020), 103514. https://doi.org/10.1016/j.rinp.2020.103514
16. E. M. E. Zayed, H. A. Zedan, K. A. Gepreel, Group analysis and modified extended Tanh-function to find the invariant solutions and soliton solutions for nonlinear Euler equations, *Int. J. Nonlinear Sci. Num. Simul.*, **5** (2004), 221–234. https://doi.org/10.1515/IJNSNS.2004.5.3.221
17. A. Biswas, D. Milovic, Travelling wave solutions of the non-linear Schrödinger's equation in non-Kerr law media, *Commun. Nonlinear Sci. Num. Simul.*, **14** (2009), 1993–1998. https://doi.org/10.1016/j.cnsns.2008.04.017
18. A. Aasaraai, The application of modified F-expansion method for solving the Maccari's system, *Brit. J. Math. Comput. Sci.*, **11** (2015), 1–14.

19. E. Fan, Extended tanh-function method and its applications to nonlinear equations, *Phys. Lett. A*, **277** (2000), 212–218. https://doi.org/10.1016/S0375-9601(00)00725-8

20. Z. S. Feng, The first-integer method to study the Burgers-Krotweg-de Vries equation, *J. Phys. A Math. Gen.*, **35** (2002), 343–349.

21. V. B. Matveev, M. A. Salle, *Darboux transformations and solitions*, Berlin, Heideelberg: Springer, 1991.

22. M. S. Islam, K. Kamruzzaman, M. A. Akbar, A. Mastroberardino, A note on improved F-expansion method combined with Riccati equation applied to nonlinear evolution equations, *R. Soc. Open Sci.*, **1** (2014), 1–13. https://doi.org/10.1098/rsos.140038

23. L. Akinyemi, M. Şenol, H. Rezazadeh, H. Ahmad, H. Wang, Abundant optical soliton solutions for an integrable (2+1)-dimensional nonlinear conformable Schrödinger system, *Results Phys.*, **25** (2021), 104177. https://doi.org/10.1016/j.rinp.2021.104177

24. M. A. Akbar, L. Akinyemi, S. W. Yao, A. Jhangeer, H. Rezazadeh, M. M. A. Khater, et al., Soliton solutions to the Boussinesq equation through sine-Gordon method and Kudryashov method, *Results Phys.*, **25** (2021), 104228. https://doi.org/10.1016/j.rinp.2021.104228

25. L. Akinyemi, K. Hosseini, S. Salahshour, The bright and singular solitons of (2+1)-dimensional nonlinear Schrödinger equation with spatio-temporal dispersions, *Optik*, **242** (2021), 167120. https://doi.org/10.1016/j.ijleo.2021.167120

26. L. Akinyemi, H. Rezazadeh, S. W. Yao, M. A. Akbar, M. M. A. Khatere, A. Jhangeer, et al., Nonlinear dispersion in parabolic law medium and its optical solitons, *Results Phys.*, **26** (2021), 104411. https://doi.org/10.1016/j.rinp.2021.104411

27. M. Mirzazadeh, A. Akbulut, F. Taşcan, L. Akinyemi, A novel integration approach to study the perturbed Biswas-Milovic equation with Kudryashov's law of refractive index, *Optik*, **252** (2022), 168529. https://doi.org/10.1016/j.ijleo.2021.168529

28. A. Kilicman, R. Shokhanda, P. Goswami, On the solution of (n+1)-dimensional fractional M-Burgers equation, *Alex. Eng. J.*, **60** (2021), 1165–1172. https://doi.org/10.1016/j.aej.2020.10.040

29. R. Shokhanda, P. Goswami, J. H. He, A. Althobaiti, An approximate solution of the time-fractional two-mode coupled Burgers equation, *Fractal Fract.*, **5** (2021), 1–18. https://doi.org/10.3390/fractalfract5040196

30. C. L. Yuan, X. Y. Wen, Soliton interactions and asymptotic state analysis in a discrete nonlocal nonlinear self-dual network equation of reverse-space type, *Chinese Phys. B*, **30** (2021), 030201.

31. H. T. Wang, X. Y. Wen, Modulational instability, interactions of two-component localized waves and dynamics in a semi-discrete nonlinear integrable system on a reduced two-chain lattice, *Eur. Phys. J. Plus*, **136** (2021), 1–43. https://doi.org/10.1140/epjp/s13360-021-01454-4

32. C. L. Yuan, X. Y. Wen, Integrability, discrete kink multi-soliton solutions on an inclined plane background and dynamics in the modified exponential Toda lattice equation, *Nonlinear Dyn.*, **105** (2021), 643–669. https://doi.org/10.1007/s11071-021-06592-z

33. X. Y. Wen, H. T. Wang, Breathing-soliton and singular rogue wave solutions for a discrete nonlocal coupled Ablowitz-Ladik equation of reverse-space type, *Appl. Math. Lett.*, **111** (2021), 106683. https://doi.org/10.1016/j.aml.2020.106683

34. X. Wang, C. Liu, L. Wang, Darboux transformation and rogue wave solutions for the variable-coefficients coupled Hirota equations, *J. Math. Anal. Appl.*, **449** (2017), 1534–1552. https://doi.org/10.1016/j.jmaa.2016.12.079

35. X. Wang, L. Wang, J. Wei, B. W. Guo, J. F. Kang, Rogue waves in the three-level defocusing coupled Maxwell-Bloch equations, *Proc. R. Soc. A*, **477** (2021), 1–21. https://doi.org/10.1098/rspa.2021.0585

36. Y. S. Tao, J. S. He, Multisolitons, breathers, and rogue waves for the Hirota equation generated by the Darboux transformation, *Phys. Rev. E*, **85** (2012), 026601.

37. C. Q. Dai, J. F. Zhang, New solitons for the Hirota equation and generalized higher-order nonlinear Schrödinger equation with variable coefficients, *J. Phys. A Math. Gen.*, **39** (2006), 723–737.

38. L. Faddeev, A. Y. Volkov, Hirota equation as an example of an integrable symplectic map, *Lett. Math. Phys.*, **32** (1994), 125–135. https://doi.org/10.1007/BF00739422

39. X. Wang, C. Liu, L. Wang, Darboux transformation and rogue wave solutions for the variable-coefficients coupled Hirota equations, *J. Math. Anal. Appl.*, **449** (2017), 1534–1552. https://doi.org/10.1016/j.jmaa.2016.12.079

40. K. El-Rashidy, A. R. Seadawy, S. Althobaiti, M. M. Makhlouf, Multiwave, Kinky breathers and multi-peak soliton solutions for the nonlinear Hirota dynamical system, *Results Phys.*, **19** (2020), 103678. https://doi.org/10.1016/j.rinp.2020.103678

41. R. Hirota, Exact envelope-soliton solutions of a nonlinear wave equation, *J. Math. Phys.*, **14** (1973), 805–809. https://doi.org/10.1063/1.1666399

42. P. Wang, B. Tian, W. J. Liu, M. Li, K. Sun, Soliton solutions for a generalized inhomogeneous variable-coefficient Hirota equation with symbolic computation, *Stud. Appl. Math.*, **125** (2010), 213–222. https://doi.org/10.1111/j.1467-9590.2010.00486.x

43. G. Jumarie, Modified Riemann-Liouville derivative and fractional Taylor series of nondifferentiable functions further results, *Comput. Math. Appl.*, **51** (2006), 1367–1376. https://doi.org/10.1016/j.camwa.2006.02.001

44. A. Scott, *Encyclopedia of nonlinear science*, New York: Routledge, 2005. https://doi.org/10.4324/9780203647417

45. A. Atangana, D. Baleanu, New fractional derivatives with nonlocal and non-singular kernel: Theory and application to heat transfer model, *Therm. Sci.*, **20** (2016), 763-769. https://doi.org/10.2298/TSCI160111018A

46. A. Kurt, A. Tozar, O. Tasbozan, Applying the new extended direct algebraic method to solve the equation of obliquely interacting waves in shallow waters, *J. Ocean Univ. China*, **19** (2020), 772–780. https://doi.org/10.1007/s11802-020-4135-8

AIMS Press